



Published in final edited form as:

Circ Res. 2017 February 17; 120(4): 701–712. doi:10.1161/CIRCRESAHA.116.309935.

Experimental, Systems and Computational Approaches to Understanding the MicroRNA-Mediated Reparative Potential of Cardiac Progenitor Cell-Derived Exosomes From Pediatric Patients

Udit Agarwal^{1,2}, Alex George¹, Srishti Bhutani¹, Shohini Ghosh-Choudary¹, Joshua Maxwell^{1,2}, Milton E. Brown^{1,2}, Yash Mehta¹, Manu O. Platt¹, Yaxuan Liang⁴, Susmita Sahoo⁴, and Michael E. Davis^{1,2,3,*}

¹Wallace H. Coulter Department of Biomedical Engineering, Emory University and Georgia Institute of Technology, Atlanta, GA

²Division of Cardiology, Emory University School of Medicine, Atlanta, GA

³Children's Heart Research and Outcomes Center, Emory University School of Medicine and Children's Healthcare of Atlanta, Atlanta, GA

⁴Icahn School of Medicine, Mount Sinai, New York, NY

Abstract

Rationale—Studies have demonstrated that exosomes can repair cardiac tissue post myocardial infarction (MI) and recapitulate the benefits of cellular therapy.

Objective—We evaluated the role of donor age and hypoxia of human pediatric cardiac progenitor cell (CPC)-derived exosomes, in a rat model of ischemia reperfusion (IR) injury.

Methods and Results—Human CPCs from the right atrial appendages from children of different ages undergoing cardiac surgery for congenital heart defects were isolated and cultured under hypoxic or normoxic conditions. Exosomes were isolated from the culture-conditioned media and delivered to athymic rats following IR injury. Echocardiography at day-3 post-MI suggested statistically improved function in neonatal hypoxic and neonatal normoxic groups compared to saline-treated controls. At 28 days post-MI exosomes derived from neonatal normoxia, neonatal hypoxia, infant hypoxia, and child hypoxia significantly improved cardiac function compared to saline-treated controls. Staining showed decreased fibrosis and improved angiogenesis in hypoxic groups compared to controls. Finally, using sequencing data, a computational model was generated to link microRNA levels to specific outcomes.

Address correspondence to: Dr. Michael E. Davis, Associate Professor of Biomedical Engineering, 1760 Haygood Drive, W200, Atlanta, GA 30322, Tel: (404) 727-9858, michael.davis@bme.emory.edu.

DISCLOSURES

None.

AUTHOR CONTRIBUTIONS

UA, MED designed the research. UA, AG, SB, SGC, MEB, YL, YM performed research. MOP and SS contributed analytical tools. UA, AG and MED analyzed data. UA, and MED wrote the paper.

Conclusion—CPC exosomes derived from neonates improved cardiac function independent of culture oxygen levels, while CPC-exosomes from older children were not reparative unless subjected to hypoxic conditions. Cardiac functional improvements were associated with increased angiogenesis, reduced fibrosis and improved hypertrophy resulting in improved cardiac function; however, mechanisms for normoxic neonatal CPC exosomes improved function independent of those mechanisms. This is the first study of its kind demonstrating that donor age and oxygen content in the microenvironment significantly alter the efficacy of human CPC-derived exosomes.

Keywords

Cardiac progenitor cells; microRNA; modeling; systems biology; exosome

Subject Terms

Basic Science Research; Cell Therapy; Computational Biology; Stem Cells

INTRODUCTION

Approximately 7.3 million people die of ischemic heart disease globally every year and almost 1 in every 6 deaths occurs in the United States due to cardiovascular disease¹. Multiple modalities of therapies have been under investigation for improving cardiac function post myocardial infarction (MI) and preventing onset of heart failure. For the last two decades, stem cell therapy has become an exciting potential for therapy for improved cardiac remodeling post-MI. While initially thought to be directly the contribution of cells themselves, the majority of researchers now believe paracrine mechanisms are likely the benefit of cell therapy. This holds true for many cell types including but not limited to mesenchymal, hematopoietic, and cardiac-derived.

Cardiac progenitor cells (CPCs, sometimes referred to as cardiac stem cells) were discovered in 2003² and studies have shown that these cells may contribute to cardiac turnover after injury. Initially it was thought that direct differentiation of cardiac stem cells into cardiac myocytes was responsible for improved remodeling; however, as the science progressed, it became more evident that paracrine effects play a major role in the beneficial effects observed after CPC therapy³. Despite the data that suggest that CPCs do not form new myocytes, clinical trials involving CPCs⁴ and other cardiac-derived cells such as cardiosphere-derived cells (CDCs)⁵⁻⁷ show modest benefits in the clinic. Despite the clinical advances, mechanisms for recovery are still under investigation.

Exosomes have gathered a growing interest recently when it was determined that they carry mRNAs and microRNAs which contribute towards intercellular signaling⁸. Since these important findings, few studies have been published documenting the important role of exosomal driven myocardial healing post-MI including a recent study from our group which showed that rat CPCs make exosomes and culturing cells under hypoxic conditions changes microRNA content and improves post-MI repair⁹. Furthermore, CDC-derived exosomes also improve ventricular remodeling and exert anti-fibrotic, angiogenic and anti-apoptotic response on the myocardial healing¹⁰. Finally, recent studies suggest that exosomes derived

from several different cell types improve myocardial repair, including mouse embryonic stem cells¹¹ and human CD34+ stem cells¹². Adding to the importance of exosomes, a recent study demonstrated that blockade of exosome secretion decreased the benefits of CDC therapy¹³, establishing the involvement of paracrine secretion from stem cells in cardiac repair.

During embryogenesis, all the cells of a developing fetus including stem cells grow in a relative hypoxic environment suggesting that hypoxia induces regenerative effects¹⁴. Moreover, we have recently shown that younger CPCs have more beneficial effects compared to older CPCs as their efficacy decreases by the time the child reaches 1 year of age¹⁵. Based upon these observations we hypothesized that exosomes derived from hypoxic and neonatal CPCs can improve ventricular remodeling post-MI. In this report we tested the effect of donor age and hypoxia on exosomes derived from various pediatric age group CPCs (neonates, infant and child) in ventricular remodeling post MI. We then used computational modeling, incorporating studies using other human cell types to strengthen our model, to predict potential mediators.

METHODS

Human sample acquisition and isolation of c-kit-positive hCPCs

This study was approved by the Institutional Review Board at Children's Healthcare of Atlanta and Emory University. Approximately 70–100 mg of right atrial appendage tissue was obtained from children with varied congenital heart diseases, undergoing reconstructive heart surgeries. Human c-kit positive CPCs were isolated and characterized as described previously¹⁵. In brief, right atrial appendages of the children undergoing cardiac surgeries for various reasons were isolated and transported using Krebs-Ringer solution containing 35 mmol/L NaCl, 4.75 mmol/L KCl, 1.2 mmol/L KH₂PO₄, 16 mmol/L Na₂HPO₄, 134 mmol/L sucrose, 25 mmol/L NaHCO₃, 10 mmol/L glucose, 10 mmol/L HEPES, and 30 mmol/L 2,3butanedionemonoxime, pH7.4, with NaOH. The appendages were minced and were digested using collagenase type 2 from Worthington (300 U/ml). The digested tissue was filtered and cells were pelleted by centrifuging at 1000×g for 5 min. The cells were then mixed with beads coated with anti-c-kit antibody (Santa Cruz H300) followed by magnetic sorting (MACS) and washes with media. Cells were grouped in to 3 age groups for the studies as follows: neonate (0–1 months), infant (1–12 months), child (2–5 years).

Media components

CPCs were cultured in media that consisted of Hams F12 medium supplemented with 50 ml of fetal bovine serum (FBS), 5 ml of antibiotic and antimycotic, 5 ml of L-glutamine and 200 µl of human fibroblast growth factor-2 (25 mg/ml). CPC quiescent and treatment media consisted of Hams F12 medium supplemented with 1% antibiotic (5 ml) and antimycotic, 1% L-glutamine (5 ml) neither FBS nor bFGF were used. Cardiac endothelial cells were cultured in complete rat endothelial cell medium from Cell Biologic (Cat #M1266) containing 0.5 ml EGF, 0.5 ml VEGF, 5 ml L-glutamine, 5 ml antibiotic-antimycotic solution and 10 ml FBS. Cardiac fibroblast media fibroblasts consisted for 50ml of FBS, 5

ml of L-glutamine, 5 ml of penicillin, and 5 ml of streptavidin in DMEM. All final media volumes were 500 mL.

Generation and isolation of exosomes

Pediatric hCPCs were quiesced in serum free media for 12 hours followed by a media change and either normoxic or 1% oxygen conditions for another 12 hours. Conditioned media was collected and pooled from 3 separate individual patient cell lines per age range for 3 passages to reduce variability. The conditioned media was subjected to multiple ultracentrifugation steps using Optima XPN-100 Ultracentrifuge (Beckman Coulter) and exosomes were collected. In brief, the conditioned media was centrifuged at 7500 rpm for 5 min at 4°C to pellet the debris, followed by 2 washes in PBS at 24000 rpm for 70 min at 4°C. The exosome pellet was isolated and the protein content of the exosomes was analyzed by Micro BCA Protein Assay kit (Thermo Scientific Pierce 23235) according to the manufacturer's instructions. Transmission Electron Microscopy (JEOL JEM – 1400) was used to determine the presence as well as the size of the exosomes.

Exosome labeling with Acridine Orange and uptake study

Exosomes were labeled with acridine orange (AO) as described⁹. In brief 500 µmol/L AO stock was prepared in autoclaved water and combined with 4 µg of exosomes (diluted in PBS) in a 1:24 ratio to yield 2 mL of sample with an AO concentration of 20 µmol/L. The sample was incubated at room temperature for 90 minutes. Subsequent dialysis in PBS was performed at 4°C with buffer changes at 2 and 4 hours before leaving the sample in buffer overnight. The labeled exosomes were covered and stored at –80 °C. For the uptake study, rat adult cardiac myocytes, rat cardiac fibroblasts and rat cardiac endothelial cells were incubated with 1 µg of labeled exosomes for 2 hours. Nuclei were stained with Hoescht and live cell imaging was performed using an Olympus Fluoview FV-1000 confocal microscope (Olympus, Melville, NY). Fluorescence was analyzed using Image J.

Animal surgery

All animal experiments were performed with the approval of the Institutional Animal Care and Use Committee of Emory University. Athymic rats (CrI:NIH-*Foxn1^{tmu}*) (~250gm) were obtained from Charles River Laboratory. Rats were anesthetized with 2% of isoflurane (Isolurane, USP Piramal Healthcare), orally intubated, and ventilated. The left anterior descending coronary artery was ligated for 30 mins followed by reperfusion. Exosomes (80 µg/kg suspended in 100 µL of PBS) were injected into the myocardium at 3 different sites of the border zones in a randomized and double-blinded manner. 2D echocardiography was performed at day 3 and 28 post MI (Acuson Sequoia 512 with a 14 MHz transducer). All functional evaluations were conducted and analyzed by investigators blinded to the animal's treatment group. After 28 days, the rats were euthanized and the hearts were excised for histological analysis. The hearts were fixed in formalin followed by paraffin embedding.

Picrosirius staining

Collagen staining was done as described¹⁵. In brief, the paraffin embedded sections were dewaxed using histoclear (10 min X 2). Multiple ethanol washes were performed in series

followed by 1-hour incubation with picosirius red solution (Sigma). The sections were washed with acetic acid for 45 min followed by 100% ethanol for 1 min, and finally mounted with resinous medium (Cytoseal). Images were taken using a slide scanner - Hamamatsu Nanozoomer 2.0HT. Percent fibrosis of the LV was quantified using Aperio Imagescope v12.1.0.5029 software. The LV wall was traced, excluding the pericardium and a line was drawn bisecting the muscular septum equally to calculate the LV region. The percent fibrosis was quantified using strong positive signal divided by total signal.

Immunostaining

Rats were sacrificed at day 28 post-treatment. Hearts were harvested and fixed in formalin followed by paraffin embedding. Capillary and cell membrane staining was performed as described. In brief, paraffin wax was removed from the 7 μ m tissue sections using histoclear (10 min \times 2) followed by various ethanol washes. Antigen retrieval was performed using sodium citrate (10 mmol/L) followed by blocking with 2% BSA. For capillary staining, tissue sections were incubated overnight with Isolectin GS-IB4, Alexafluor 647 conjugate from Life Technologies (1:25 dilution) at 4°C. Cell membrane staining was performed using Rhodamine-conjugated wheat germ agglutinin (WGA) from Vector Laboratories (RL1022, 1:250 dilution).

Hypertrophy analysis

Two-dimensional echocardiography was used to quantify the posterior wall thickness. The m-mode quantification of posterior wall thickness was measured at mid-papillary level for various groups. Histological assessment of hypertrophy was performed by labeling myocyte borders with WGA. The cross section of at least 15 myocytes per field in the peri-infarct zone with centrally placed nucleus was quantified and averaged. A sample histogram from one sham and one IR animal is shown as Supplemental Figure I.

Infarct sizing

Myocardial infarct size was evaluated using 2,3,5-triphenyltetrazolium chloride (TTC) staining and Evans Blue dye in which the percent area of infarction was calculated as the infarcted area (TTC stained) divided by the ischemic area at risk. Cytokine analysis and infarct size were performed at 24 hours following reperfusion.

microRNA array analysis

Exosomes were isolated from 3 individual hCPC cell lines belonging to children with 3 different age groups and then pooled to form neonate, infant and child exosomes. RNA was extracted and whole gene and microRNA array was performed using Affymetrix microRNA arrays were by the Emory Integrated Genomics Core. Principal component (PC) and partial least squares regression (PLSR) analysis were performed using the SIMCA-P software (UMetrics) that solves the partial least squares regression (PLSR) problem with the nonlinear partial least squares algorithm.

Statistical analysis

Statistics were calculated with GraphPad Prism software as described in the legends. Unpaired t-test was used where appropriate. One way ANOVA was used with Tukey's post-test when multiple groups were compared.

RESULTS

Exosomal uptake in cardiac cells

Isolated CPC-exosomes were generated as described and were visualized using transmission electron microscopy (Figure 1A). The size of the exosomes did not vary in between the hypoxic and normoxic groups and was determined to be 120 ± 12 nm. Exosomes were labeled with acridine orange and the various cardiac cell types (rat cardiac myocytes, rat fibroblast and rat endothelial cells) were incubated for 2 hours to determine uptake. Our results demonstrate that the exosomes are taken up by target cells at varying levels. All 3 major cardiac cell types (fibroblast, endothelial, cardiomyocytes) internalized labeled exosomes, though there were cell specific differences. Cardiac myocytes internalized exosomes to a very minimal extent (Figure 1B). More uptake was seen in endothelial cells (Figure 1C) and maximal uptake was seen in fibroblasts (Figure 1D). Data were quantified in Supplemental Figure II. We further tested if the minimal uptake of exosomes in cardiac myocytes resulted in any phenotypic changes by performing sarcomere shortening and calcium transient measurements however we found no significant changes in the cardiac myocytes treated with either normoxic and hypoxic exosomes compared to controls (Supplemental Figure III).

Hypoxic and neonate CPCs derived exosomes improve cardiac function

Twenty μ g of CPC-exosomes were delivered to athymic rats after 30 mins of ischemia-reperfusion (IR) injury. These rats were followed for 28 days and ejection fraction (EF) was recorded at day 3 and day 28 post-IR. At day 3 post-IR, our results demonstrate a statistically significant improved EF in athymic rats treated with either neonatal normoxia or neonatal hypoxia exosomes compared with the controls. CPC-exosomes isolated from other older groups including infant and child, isolated from either normoxic and hypoxic cultures did not significantly improve the EF compared to the IR controls (Figure 2A). Interestingly at day 28 post MI, neonatal normoxia and hypoxia groups retained their improved EFs, however infant and child CPC-exosomes from hypoxic, but not from normoxic cultures resulted in statistically significant improvement of EF compared to the control (Figure 2B).

Hypoxic CPCs derived exosomes improved fibrosis and angiogenesis

To further decipher the mechanisms responsible for improved ejection fraction as described above, we examined fibrosis and angiogenesis in the infarcted region. Picrosirius red collagen staining was performed to determine the collagen content at day 28 post-IR. The percent collagen content was analyzed at the level of papillary muscles. Our results demonstrate that the athymic rats treated with hypoxic exosomes from various age groups showed significantly decreased fibrosis compared to their normoxic counterparts as well as

the IR control animals. Interestingly, despite improved cardiac function, the neonatal normoxic CPC-exosomes treatment had no improvement in fibrosis (Figure 3).

We further analyzed the angiogenesis within the infarcted region of the heart. Isolectin staining was performed to label the capillaries and counting was performed at 3 different places within the infarcted region. Our results show that angiogenesis was significantly improved among the hypoxic exosome groups compared to their normoxic counterparts and IR control animals (Figure 4) suggesting treatment of hypoxic CPC-exosomes have a beneficial effect in ventricular remodeling. Consistent with fibrosis, neonatal normoxic CPC-exosomes had no significant effect on angiogenesis.

CPCs derived exosomes improve hypertrophy

To determine the effect of CPC-exosomes on hypertrophy of the cardiac myocytes, histological as well as echocardiographic measurements were performed. We analyzed peri-infarct hypertrophy histologically, by measuring the cross sections of cardiac myocytes at the level of a visible nucleus (stained with DAPI) at 3 different peri-infarct locations within the myocardium of all the groups. The cardiac myocyte cell membranes were labeled with WGA (Figure 5A). Our results demonstrate that irrespective of age and oxygen content of the culture environment, CPC-derived exosomes decrease peri-infarct hypertrophy significantly (Figure 5B) compared to IR controls. We further analyzed the remote hypertrophy by measuring left ventricular posterior wall diameter (LVPWd) at day 28 post-IR by 2D echo. Interestingly our results demonstrate that relatively younger groups including neonatal and infant hypoxic CPC-exosomes had statistically improved LVPWd compared with IR controls. Furthermore, hypoxic CPC exosome treatment significantly improved LVPWd compared to normoxic CPC exosomes; however, no significant differences were observed in between the other hypoxic and normoxic groups (Figure 5C).

Computational modeling of microRNAs

To predict the mechanisms responsible for these observed outcomes, we used an approach of principal component analysis (PCA) and partial least squares regression (PLSR). We have used this approach in the past to establish relationships between covariant microRNAs within CPCs and exosomes and their regenerative effects. For this study we performed whole microRNA array from the exosomes derived from 3 individual patients in each group to establish a relationship between donor CPC age and environment (cues), microRNAs (signals), and responses of EF at day 3 and 28, angiogenesis, and fibrosis using PLSR. PC scores plot illustrates tight clustering in PC space by age as well as hypoxia (Figure 6A). Variable importance of projection (VIP) calculations determined each microRNA signal's contribution to an outcome. Of the top 100 microRNAs, we used miRTarBase to isolate microRNAs with known targets (by at least 3 assays). Our analysis returned 32 microRNAs, which were then plotted in PC space with outcomes (Figure 6B).

Validation of our computational model

As several other studies have shown a benefit of exosomes and performed sequencing, we created a predictive model to determine whether we could use data from other studies to test and enhance our model. We chose data from a study on CD34+ cells as they showed a

similar phenotype (angiogenesis), were human-derived, and complete microRNA sequencing was available¹². Using this combined data, we made predictive models shown in Figure 7A using our top 30 microRNAs. This model had very high predictability for angiogenesis and slightly less so for other functions, as that paper did not measure cardiac function or fibrosis. As the graph in Figure 7B shows, we were able to predict (white bars) data from the paper (black) with a high degree of fidelity. We then replotted all array data in PC space (Figure 7C) and show tight clustering of CD34+ cell-derived exosomes with exosomes derived from newborns. Finally, in Figure 7D, we created a new PLSR model using all microRNA data from both studies, to predict common microRNAs from both studies that contribute to the reparative phenotype. As our predictive model only took in to account the top microRNAs, we made another predictive model using the complete dataset of microRNAs so it may be more generalizable (Supplemental Figure III).

Neonate CPCs derived exosomes have acute cardioprotective effects

As our results showed that neonate CPCs derived exosomes improved EF at day 3 and 28 post IR, we evaluated their acute effect on infarct size and potential mechanisms by performing TTC staining and evaluating expression of various cytokines in the tissue using Luminex expression analysis, respectively. Our results demonstrate that although there was a 25% reduction in infarct size of rats treated with normoxic-derived neonatal CPCs exosomes, no statistical difference between the control (IR + saline only) and neonatal normoxic CPCs exosome group, was observed. In contrast, hypoxia-derived neonate CPCs exosomes significantly ($p < 0.05$) reduced the infarct size (Figure 8) suggesting an acute beneficial effect in addition to the improved angiogenesis and decreased fibrosis. We further analyzed potential mechanisms of these observed effects by quantifying the cytokine content using Luminex analysis. Our results show that IL-6 was significantly reduced in rats treated with hypoxia-derived neonate exosomes, and to a smaller degree IL-1 α (not significantly decreased). In addition, IL-18 levels were significantly upregulated in the rats treated with neonate CPCs derived exosomes (and to a lesser degree IL-10; Supplemental Figure V).

DISCUSSION

Since their discovery in 2003, CPC therapy has rapidly advanced to clinical trials without complete understanding of mechanisms involved. While once thought to be direct cardiac differentiation of these cells, it is now widely accepted that the beneficial effects of CPCs are driven via paracrine mechanisms including secretion of cytokines and vesicles into the extracellular space. Recently exosomes have moved to the forefront of potential paracrine mediators due to their ability to carry microRNAs and influence local gene expression. Multiple groups including our laboratory have published that progenitor cells produce exosomes carrying microRNAs that can improve ventricular remodeling. In this study we found that human pediatric CPCs generate exosomes with the size of 120 ± 12 nm, similar to what is reported in literature^{16, 17}.

A recent study showed that human CPCs derived extracellular vesicles reproduced the similar beneficial effects compared to their parent cell in chronic heart failure model¹⁸. While interesting, this study looked at embryonic stem cell-derived CPCs and not isolated

from tissue. Additionally, exosomes were not separated from the total extracellular vesicle content. Nonetheless, the current study builds on this one, as well as our prior study of rat CPC-derived exosomes. There are reports of exosomes from many cell types improving cardiovascular repair including CD34+ cells^{12, 19, 20}, CDCs^{10, 13}, embryonic stem cells^{11, 21}, and mesenchymal stem cells^{22, 23}. While the potential mechanisms may differ slightly, all of these exosomes show improvements in similar outcomes including fibrosis, angiogenesis, and cardiac function, suggesting some potential common mechanisms. What these data do show, which is rather interesting, is that many of the benefits of cell therapy can be recapitulated without the cells themselves. This is important for sources such as embryonic stem cells, which have tumorigenicity concerns that showed no tumorigenicity of exosomes¹¹, and may alleviate the concerns of many other cells. Moreover, as exosomes, as cell free sources, have the potential to be allogeneic therapy. This could mean a single optimal source could be obtained and standardized, another important limitation of cell therapy.

Our study also demonstrates that all 3 major cardiac cell types (fibroblast, endothelial, cardiomyocytes) internalize human pediatric CPCs as shown by confocal imaging of acridine orange-labeled exosomes. There were cell-specific differences with fibroblasts taking up the most exosomes, followed by endothelial cells; however, cardiomyocytes minimally internalized exosomes. While studies have suggested that myocytes produce exosomes^{24, 25}, this is the first report of cardiac myocytes internalizing exosomes. Despite this, many studies show improvements in cardiac function without any particular effect on myocytes themselves, including some from our laboratory. Furthermore, a recent study by Tselieu et al showed that fibroblast cells primed with CDC derived exosomes exhibited anti-fibrotic, anti-apoptotic and angiogenic effects, suggesting that uptake of exosomes by fibroblast cells may be enough to drive the regenerative/repairative process¹⁰. Regardless, this minimal uptake of exosomes by cardiomyocytes produced very little functional effects on the myocytes themselves.

Our study is an attempt to understand the role hypoxia and age of the CPCs play in modulating the effect of exosomes generated from these cell types. We observe that neonatal exosomes irrespective of the environment have improved ventricular function at day 3 and day 28 post-IR. This earlier preservation of cardiac function at day 3, along with our finding that exosomes from neonatal cells under normoxia improved function independent of fibrosis and angiogenesis, suggest an interplay of a single or multiple acute mechanisms. Given our findings that exosomes are not taken up by cardiomyocytes, we speculate that actions on local fibroblasts, or perhaps even infiltrating inflammatory cells, could improve myocyte survival. Moreover, we do not rule out the possibility of exosome-reprogrammed fibroblasts and endothelial cells modulating the cardiomyocyte function via secretion of potent endogenous exosomes taken up by myocytes. This remains a very interesting area for future studies.

We also analyzed cardiac myocyte hypertrophy among these groups in the peri-infarct zone histologically. Our data demonstrates that all the groups had decreased peri-infarct hypertrophy compared to the controls, suggesting that even the exosomes generated in the normoxic conditions might have some beneficial role; although not physiologically relevant.

Interestingly on measuring the LVPWd, we found that hypoxic exosomes from neonate CPCs had the significantly decreased hypertrophy compared with their normoxic counterparts and control animals. Furthermore, hypoxic exosomes from infant CPCs also had improved hypertrophy compared with controls but not with their normoxic counterparts. These results suggest that although the phenotypes of child and infant exosomes are similar, small intricacies and disparities still exist.

Recently our laboratory showed that the efficacy of rat-derived CPC exosomes increases after subjecting cells to hypoxia. Moreover, the microRNA content in the hypoxic exosomes also changed with hypoxia, suggesting that possible compensatory pathways exist in the CPCs to alter secretion based upon microenvironmental cues⁹. While the mechanism for this is unclear, it could be possible that pathways involving proteins such as hypoxia inducible factor-1 play a role. Our results also demonstrate that hypoxia reverses the phenotype of infant and child CPC-derived exosomes as we observed improved remodeling via increased angiogenesis and decreased fibrosis, suggesting another therapeutic approach in increasing the quality of these exosomes. As our recent study showed donor age-dependent effect of cells in response to right ventricular overload repair¹⁵, it is possible that hypoxia could alter the reparative phenotype of these cells as well.

To predict the molecular mechanisms responsible for the observed findings we took a computational biology approach. MicroRNA analysis revealed an age and hypoxia-dependent clustering of the different hCPCs derived exosomes. PC analysis showed few differences between microRNAs from neonate cells in response to hypoxia, which is interesting considering outcomes were not considered in this initial analysis. At baseline (normoxia), exosome microRNA clusters very uniquely by age, suggesting very specific age-related differences. Hypoxia brings infant and children-derived exosomes in to a different quadrant, suggesting potential covarying changes occurring that are hypoxia-specific. PLSR analysis gave quantitative outputs to how likely each microRNA was involved in our response. Certain microRNA's identified by our analysis have been shown to regulate important function like fibrosis (miR-27a and miR-29c^{26, 27}), cardiac hypertrophy (miR-29c²⁸, miR-96^{29, 30}, miR-182^{31, 32} and miR-185³³), angiogenesis (miR-27a³⁴), and apoptosis (miR-138^{35, 36}, miR-25³⁷). Although, our model is predictive of microRNA-based mechanism, these targets still need to be validated in the future studies. Our prior study showed that inhibition of the recipient cell RISC complex abrogated the effects of the exosomes, suggesting microRNA-mediated mechanisms, but we do not rule out the effects of any proteins or other species found in exosomes. The use of computational biology to help differentiate these signals is a powerful tool that could help bring thousands of microRNAs to a reasonable level that can be used to predict future values. We ran the miR arrays on the exosomes derived from 3 patients from each group (3 individual patients were run and data were averaged for statistics). While the number of patient samples is lower than desired, our prior study found tight clustering of signals within cells from patients within similar age groups. Additionally, the number of patients sampled is similar to prior studies to model kinase pathways. Although the ages were similar in the groups, the diagnoses and genders of the patients were different. We excluded any patient with known genetic mutations, however, many of these patients may have undiagnosed underlying genetic problems and our study did not account for that. To counter all of these issues more patient

samples need to be added to perform multi-variate analysis to account for patient-to-patient variability.

While a model of human pediatric CPCs is of great interest, expanding this model to include other reparative exosomes from other cell types would be extremely valuable. Identifying both unique and common signals that contribute to exosome function could help predict the efficacy of other exosome sources, as well as generate synthetic exosomes with selected signals. We have generated a new predictive model with our exosome data, and used published array data from CD34+ progenitor cell exosomes to refine our model and successfully predict published angiogenic data. This combined model showed that CD34+ cell-derived exosomes are predicted to behave similarly to CPC exosomes, and also provide a clearer map of potential signals that are shared between the 2 different cell types. Moreover, we examined the potential involved miRs identified with our model by Ingenuity Pathway Analysis. Potential pathways targeted by these miRs scoring the strongest included regulation of cell cycle and cell survival, giving potential insights in to future studies with combined exosome treatment (Supplemental Figure VI). We also tested several of the predicted miRs that had no published function in vitro to validate our model. As the data in Supplemental Figure VII show, all of the miRs predicted by our models to alter angiogenesis increased tube formation in transfected HUVECs (miRs-196a, -335, -518f, -532, and -548b). With many exosome papers now being published, the possibility exists to make our model even more powerful by incorporating data from other cell types and determining novel roles for unstudied miRs.

Interestingly, we also show that exosomes derived from neonates reduce infarct size, though only exosomes from cells subjected to hypoxia showed significant decreases. As normoxic exosomes improved function independent of fibrosis and angiogenesis, this reduction seen acutely could carry over to the chronic phase. In addition, we also saw changes in secreted factors. As our data show exosomes were not taken up by cardiomyocytes, understanding how local exosome uptake affects the post-infarct microenvironment is an interesting area for further examination. Our study adds on to the growing literature of exosomal reparative potential for cardiac disease and reports a novel finding of donor age-dependent effects of CPC-derived exosomes within the pediatric population. As numerous studies show the benefit of pediatric cells to adult cells, finding the optimal conditions within the pediatric population could help inform future therapeutic strategies. We also found that hypoxia could restore the reparative effect of exosomes in cells that have diminished ability to produce beneficial exosomes. Finally, we used computational modeling to examine covarying signals between the groups, simplify the large amount of data generated, and predicts the role of individual microRNAs both within our study, and from other studies as well. While these are just predicted mechanisms, it may help generate novel predictions for future studies.

Supplementary Material

Refer to Web version on PubMed Central for supplementary material.

Acknowledgments

This work was supported by grant HL124380 from the National Heart, Lung, and Blood Institute to MED and MOP, as well as award T32HL007745. The authors also wish to acknowledge the Children's Miracle Network gift to Children's Healthcare of Atlanta, as well as support from Katrina Ceccoli and the Darryl M. Ceccoli Research Fund.

This study was supported in part by the Robert P. Apkarian Integrated Electron Microscopy Core (RPAIEMC) and Emory Integrated Genomics Core, which are subsidized by the Emory College of Arts and Sciences and the Emory University School of Medicine and is one of the Emory Integrated Core Facilities. Additional support was provided by the National Center for Advancing Translational Sciences of the National Institutes of Health under award number UL1TR000454. The content is solely the responsibility of the authors and does not necessarily reflect the official views of the National Institutes of Health.

Nonstandard Abbreviations and Acronyms

AO	Acridine Orange
CDC	Cardiosphere-Derived Cell
CPC	Cardiac Progenitor Cell
EF	Ejection Fraction
IR	Ischemia/Reperfusion Injury
LV	Left Ventricle
LVPWd	Left Ventricular Posterior Wall Diameter
MI	Myocardial Infarction
PCA	Principal Component Analysis
PLSR	Partial Least Squares Regression
TTC	2,3,5-triphenyltetrazolium chloride
VIP	Variable Importance of Projection
WGA	Wheat Germ Agglutinin

REFERENCES

1. Go AS, Mozaffarian D, Roger VL, Benjamin EJ, Berry JD, Blaha MJ, Dai S, Ford ES, Fox CS, Franco S, Fullerton HJ, Gillespie C, Hailpern SM, Heit JA, Howard VJ, Huffman MD, Judd SE, Kissela BM, Kittner SJ, Lackland DT, Lichtman JH, Lisabeth LD, Mackey RH, Magid DJ, Marcus GM, Marelli A, Matchar DB, McGuire DK, Mohler ER 3rd, Moy CS, Mussolino ME, Neumar RW, Nichol G, Pandey DK, Paynter NP, Reeves MJ, Sorlie PD, Stein J, Towfighi A, Turan TN, Virani SS, Wong ND, Woo D, Turner MB. Heart disease and stroke statistics--2014 update: A report from the American Heart Association. *Circulation*. 2014; 129:e28–e292. [PubMed: 24352519]
2. Beltrami AP, Barlucchi L, Torella D, Baker M, Limana F, Chimenti S, Kasahara H, Rota M, Musso E, Urbanek K, Leri A, Kajstura J, Nadal-Ginard B, Anversa P. Adult cardiac stem cells are multipotent and support myocardial regeneration. *Cell*. 2003; 114:763–776. [PubMed: 14505575]
3. Maxeiner H, Krehbiel N, Muller A, Woitasky N, Akinturk H, Muller M, Weigand MA, Abdallah Y, Kasseckert S, Schreckenberger R, Schluter KD, Wenzel S. New insights into paracrine mechanisms of human cardiac progenitor cells. *Eur J Heart Fail*. 2010; 12:730–737. [PubMed: 20406797]

4. Chugh AR, Beache GM, Loughran JH, Mewton N, Elmore JB, Kajstura J, Pappas P, Tatooles A, Stoddard MF, Lima JA, Slaughter MS, Anversa P, Bolli R. Administration of cardiac stem cells in patients with ischemic cardiomyopathy: The scipio trial: Surgical aspects and interim analysis of myocardial function and viability by magnetic resonance. *Circulation*. 2012; 126:S54–S64. [PubMed: 22965994]
5. Makkar RR, Smith RR, Cheng K, Malliaras K, Thomson LE, Berman D, Czer LS, Marban L, Mendizabal A, Johnston PV, Russell SD, Schuleri KH, Lardo AC, Gerstenblith G, Marban E. Intracoronary cardiosphere-derived cells for heart regeneration after myocardial infarction (caduceus): A prospective, randomised phase 1 trial. *Lancet*. 2012; 379:895–904. [PubMed: 22336189]
6. Ishigami S, Ohtsuki S, Tarui S, Ousaka D, Eitoku T, Kondo M, Okuyama M, Kobayashi J, Baba K, Arai S, Kawabata T, Yoshizumi K, Tateishi A, Kuroko Y, Iwasaki T, Sato S, Kasahara S, Sano S, Oh H. Intracoronary autologous cardiac progenitor cell transfer in patients with hypoplastic left heart syndrome: The ticap prospective phase 1 controlled trial. *Circ Res*. 2015; 116:653–664. [PubMed: 25403163]
7. Tarui S, Ishigami S, Ousaka D, Kasahara S, Ohtsuki S, Sano S, Oh H. Transcoronary infusion of cardiac progenitor cells in hypoplastic left heart syndrome: Three-year follow-up of the transcoronary infusion of cardiac progenitor cells in patients with single-ventricle physiology (ticap) trial. *J Thorac Cardiovasc Surg*. 2015; 150:1198–1207. 1208, e1191–e1192. [PubMed: 26232942]
8. Valadi H, Ekstrom K, Bossios A, Sjostrand M, Lee JJ, Lotvall JO. Exosome-mediated transfer of mRNAs and microRNAs is a novel mechanism of genetic exchange between cells. *Nat Cell Biol*. 2007; 9:654–659. [PubMed: 17486113]
9. Gray WD, French KM, Ghosh-Choudhary S, Maxwell JT, Brown ME, Platt MO, Searles CD, Davis ME. Identification of therapeutic covariant microRNA clusters in hypoxia-treated cardiac progenitor cell exosomes using systems biology. *Circ Res*. 2015; 116:255–263. [PubMed: 25344555]
10. Tseliou E, Fouad J, Reich H, Slipczuk L, de Couto G, Aminzadeh M, Middleton R, Valle J, Weixin L, Marban E. Fibroblasts rendered antifibrotic, antiapoptotic, and angiogenic by priming with cardiosphere-derived extracellular membrane vesicles. *J Am Coll Cardiol*. 2015; 66:599–611. [PubMed: 26248985]
11. Khan M, Nickoloff E, Abramova T, Johnson J, Verma SK, Krishnamurthy P, Mackie AR, Vaughan E, Garikipati VN, Benedict C, Ramirez V, Lambers E, Ito A, Gao E, Misener S, Luongo T, Elrod J, Qin G, Houser SR, Koch WJ, Kishore R. Embryonic stem cell-derived exosomes promote endogenous repair mechanisms and enhance cardiac function following myocardial infarction. *Circ Res*. 2015; 117:52–64. [PubMed: 25904597]
12. Sahoo S, Klychko E, Thorne T, Misener S, Schultz KM, Millay M, Ito A, Liu T, Kamide C, Agrawal H, Perlman H, Qin G, Kishore R, Losordo DW. Exosomes from human cd34(+) stem cells mediate their proangiogenic paracrine activity. *Circ Res*. 2011; 109:724–728. [PubMed: 21835908]
13. Ibrahim AG, Cheng K, Marban E. Exosomes as critical agents of cardiac regeneration triggered by cell therapy. *Stem Cell Reports*. 2014; 2:606–619. [PubMed: 24936449]
14. Simon MC, Keith B. The role of oxygen availability in embryonic development and stem cell function. *Nat Rev Mol Cell Biol*. 2008; 9:285–296. [PubMed: 18285802]
15. Agarwal U, Smith AW, French KM, Boopathy AV, George A, Trac D, Brown ME, Shen M, Jiang R, Fernandez JD, Kogon BE, Kanter KR, Alsoufi B, Wagner MB, Platt MO, Davis ME. Age-dependent effect of pediatric cardiac progenitor cells after juvenile heart failure. *Stem Cells Transl Med*. 2016; 5:883–892. [PubMed: 27151913]
16. He M, Crow J, Roth M, Zeng Y, Godwin AK. Integrated immunoisolation and protein analysis of circulating exosomes using microfluidic technology. *Lab Chip*. 2014; 14:3773–3780. [PubMed: 25099143]
17. Lane RE, Korbie D, Anderson W, Vaidyanathan R, Trau M. Analysis of exosome purification methods using a model liposome system and tunable-resistive pulse sensing. *Sci Rep*. 2015; 5:7639. [PubMed: 25559219]
18. Kervadec A, Bellamy V, El Harane N, Arakelian L, Vanneaux V, Cacciapuoti I, Nemetalla H, Perier MC, Toeg HD, Richart A, Lemitre M, Yin M, Loyer X, Larghero J, Hagege A, Ruel M, Boulanger CM, Silvestre JS, Menasche P, Renault NK. Cardiovascular progenitor-derived

extracellular vesicles recapitulate the beneficial effects of their parent cells in the treatment of chronic heart failure. *J Heart Lung Transplant*. 2016

19. Sahoo S, Losordo DW. Exosomes and cardiac repair after myocardial infarction. *Circ Res*. 2014; 114:333–344. [PubMed: 24436429]
20. Emanuelli C, Shearn AI, Angelini GD, Sahoo S. Exosomes and exosomal miRNAs in cardiovascular protection and repair. *Vascul Pharmacol*. 2015; 71:24–30. [PubMed: 25869502]
21. Singla DK. Stem cells and exosomes in cardiac repair. *Curr Opin Pharmacol*. 2016; 27:19–23. [PubMed: 26848944]
22. Lai RC, Chen TS, Lim SK. Mesenchymal stem cell exosome: A novel stem cell-based therapy for cardiovascular disease. *Regen Med*. 2011; 6:481–492. [PubMed: 21749206]
23. Zhang Z, Yang J, Yan W, Li Y, Shen Z, Asahara T. Pretreatment of cardiac stem cells with exosomes derived from mesenchymal stem cells enhances myocardial repair. *J Am Heart Assoc*. 2016; 5
24. Malik ZA, Kott KS, Poe AJ, Kuo T, Chen L, Ferrara KW, Knowlton AA. Cardiac myocyte exosomes: Stability, hsp60, and proteomics. *Am J Physiol Heart Circ Physiol*. 2013; 304:H954–H965. [PubMed: 23376832]
25. Gupta S, Knowlton AA. Hsp60 trafficking in adult cardiac myocytes: Role of the exosomal pathway. *Am J Physiol Heart Circ Physiol*. 2007; 292:H3052–H3056. [PubMed: 17307989]
26. Marques FZ, Vizi D, Khammy O, Mariani JA, Kaye DM. The transcatheter gradient of cardiomicRNAs in the failing heart. *Eur J Heart Fail*. 2016
27. Lew WY, Bayna E, Dalle Molle E, Contu R, Condorelli G, Tang T. Myocardial fibrosis induced by exposure to subclinical lipopolysaccharide is associated with decreased mir-29c and enhanced nox2 expression in mice. *PLoS One*. 2014; 9:e107556. [PubMed: 25233448]
28. Derda AA, Thum S, Lorenzen JM, Bavendiek U, Heineke J, Keyser B, Stuhmann M, Givens RC, Kennel PJ, Schulze PC, Widder JD, Bauersachs J, Thum T. Blood-based microRNA signatures differentiate various forms of cardiac hypertrophy. *Int J Cardiol*. 2015; 196:115–122. [PubMed: 26086795]
29. Xia Y, Sheng J, Liang GY, Liu DX, Tang Q, Cheng AP. Mir-96 inhibits cardiac hypertrophy by targeting growth factor receptor-bound 2. *Genet Mol Res*. 2015; 14:18958–18964. [PubMed: 26782545]
30. Sun X, Zhang C. MicroRNA-96 promotes myocardial hypertrophy by targeting mtor. *Int J Clin Exp Pathol*. 2015; 8:14500–14506. [PubMed: 26823769]
31. Li N, Hwangbo C, Jaba IM, Zhang J, Papangeli I, Han J, Mikush N, Larrivee B, Eichmann A, Chun HJ, Young LH, Tirziu D. Mir-182 modulates myocardial hypertrophic response induced by angiogenesis in heart. *Sci Rep*. 2016; 6:21228. [PubMed: 26888314]
32. Meng Z, Wang Y, Lin Y, Nan S, Xu W, Hu B, Shen E. microRNA-182 modulates high glucose-induced cardiomyocyte hypertrophy via targeting rac1. *Zhonghua Xin Xue Guan Bing Za Zhi*. 2015; 43:619–624. [PubMed: 26420324]
33. Kim JO, Song DW, Kwon EJ, Hong SE, Song HK, Min CK, Kim do H. Mir-185 plays an anti-hypertrophic role in the heart via multiple targets in the calcium-signaling pathways. *PLoS One*. 2015; 10:e0122509. [PubMed: 25767890]
34. Zhou Q, Gallagher R, Ufret-Vincenty R, Li X, Olson EN, Wang S. Regulation of angiogenesis and choroidal neovascularization by members of microRNA-23~27~24 clusters. *Proc Natl Acad Sci U S A*. 2011; 108:8287–8292. [PubMed: 21536891]
35. Xiong H, Luo T, He W, Xi D, Lu H, Li M, Liu J, Guo Z. Up-regulation of mir-138 inhibits hypoxia-induced cardiomyocyte apoptosis via down-regulating lipocalin-2 expression. *Exp Biol Med (Maywood)*. 2016; 241:25–30. [PubMed: 26129883]
36. He S, Liu P, Jian Z, Li J, Zhu Y, Feng Z, Xiao Y. Mir-138 protects cardiomyocytes from hypoxia-induced apoptosis via mlk3/jnk/c-jun pathway. *Biochem Biophys Res Commun*. 2013; 441:763–769. [PubMed: 24211202]
37. Pan L, Huang BJ, Ma XE, Wang SY, Feng J, Lv F, Liu Y, Li CM, Liang DD, Li J, Xu L, Chen YH. Mir-25 protects cardiomyocytes against oxidative damage by targeting the mitochondrial calcium uniporter. *Int J Mol Sci*. 2015; 16:5420–5433. [PubMed: 25764156]

NOVELTY AND SIGNIFICANCE

What Is Known?

- Stem cell therapy for myocardial infarction (MI) has provided mixed results, with beneficial paracrine signaling due to exosomes being a mechanistic explanation.
- Children have a population of cardiac progenitor cells (CPCs) that reside in the heart and are thought to be beneficial, though function varies greatly with age.
- How donor age and hypoxia affect exosome quality and reparative potential is unknown.

What New Information Does This Article Contribute?

- Pediatric CPCs secrete exosomes that differ greatly in their microRNA content.
- Exosomes from newborns are reparative and efficacy decreases with age; hypoxic preconditioning of cells restores exosomal function.
- Computational modeling can create predictive models based on microRNA content and can predict function of other cellular-derived exosomes, leading to identifying new functions of microRNAs.

There is growing evidence that the benefits of stem/progenitor cell therapy are due, at least in part, to the paracrine effects of stem/progenitor cells. Most cells package intracellular bioactive molecules in exosomes, which contain surface markers that can fuse with recipient cells. This process allows for direct intracellular delivery of cellular components including microRNAs. We found that CPCs derived from children release exosomes that can repair the infarcted heart, although their efficacy decreases sharply with age. Subjecting cells to hypoxia restored reparative potential of the exosomes and changed their microRNA content. Based on computational modeling we could hypothesize which microRNAs were contributing to specific outcomes and even extend our model to other cell-derived exosomes. By analyzing microRNA data from prior studies, we were able to not only predict the function of those exosomes, but use the new data to generate hypotheses about unknown microRNA functions. Finally, we report an unbiased way to determine whether co-varying microRNAs can influence specific functions, and provide the groundwork for aggregation of data in to larger computational models to better predict and characterize exosome functions.

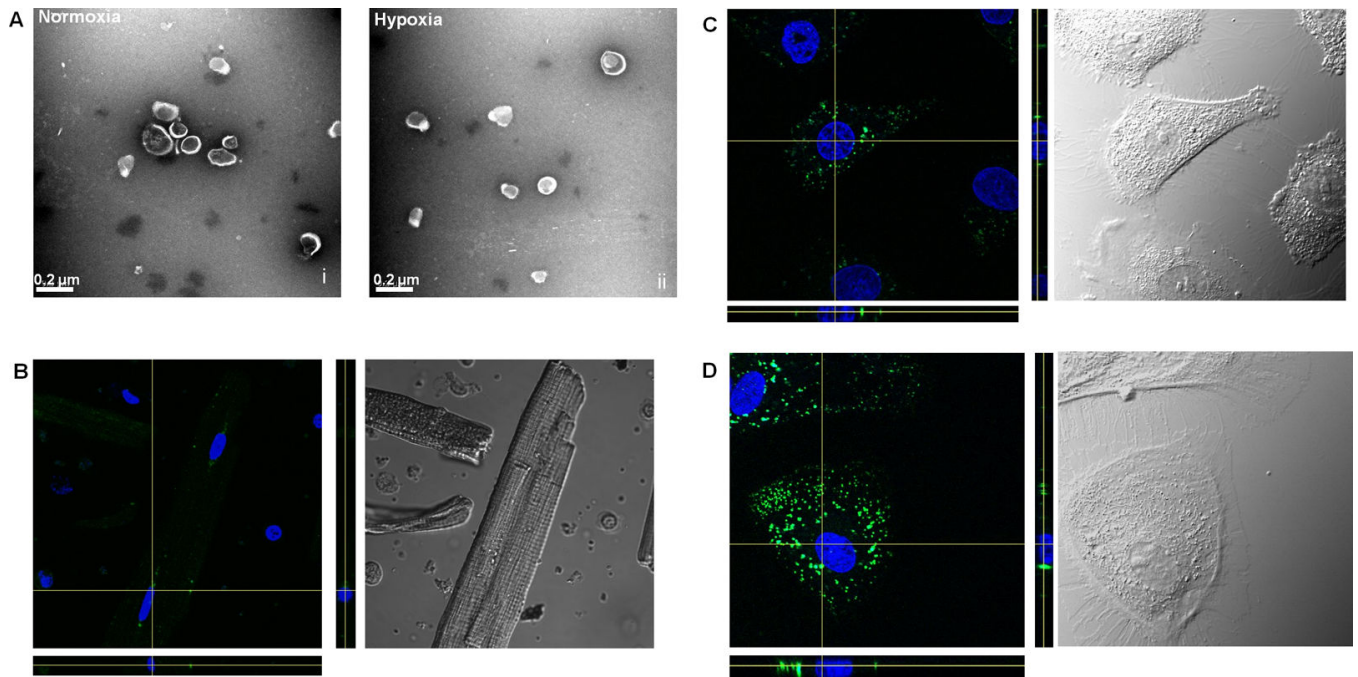


Figure 1. Characterization and exosomal uptake

A) Isolated exosomes from human pediatric CPCs were identified via Transmission Electron Microscopy. **B–D) Uptake of Exosomes** - Exosomes were taken up by the **(B)** Rat cardiac myocytes, **(C)** Rat endothelial cells and **(D)** rat cardiac fibroblast cells. Exosomes were labeled with Acridine Orange (green) and nucleus was stained with Hoechst (blue) dye. Z-stacks are given below and to the right of the confocal image.

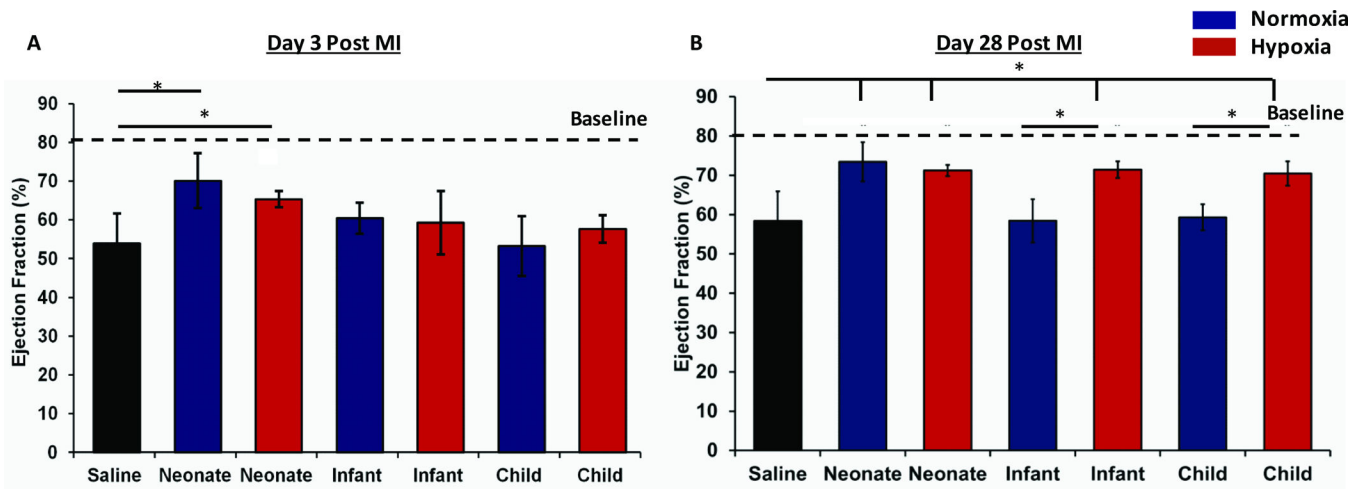


Figure 2. Functional Analysis via 2D echo

Graph represents mean \pm SEM of Ejection Fraction (%) at day 3 (**A**) and day 28 (**B**) days post MI, (n=4-5), **Blue** = Normoxia, **Red** = Hypoxia. *p < 0.05; ANOVA followed by Tukey-Kramer post-test in comparison to the saline-treated control animals.

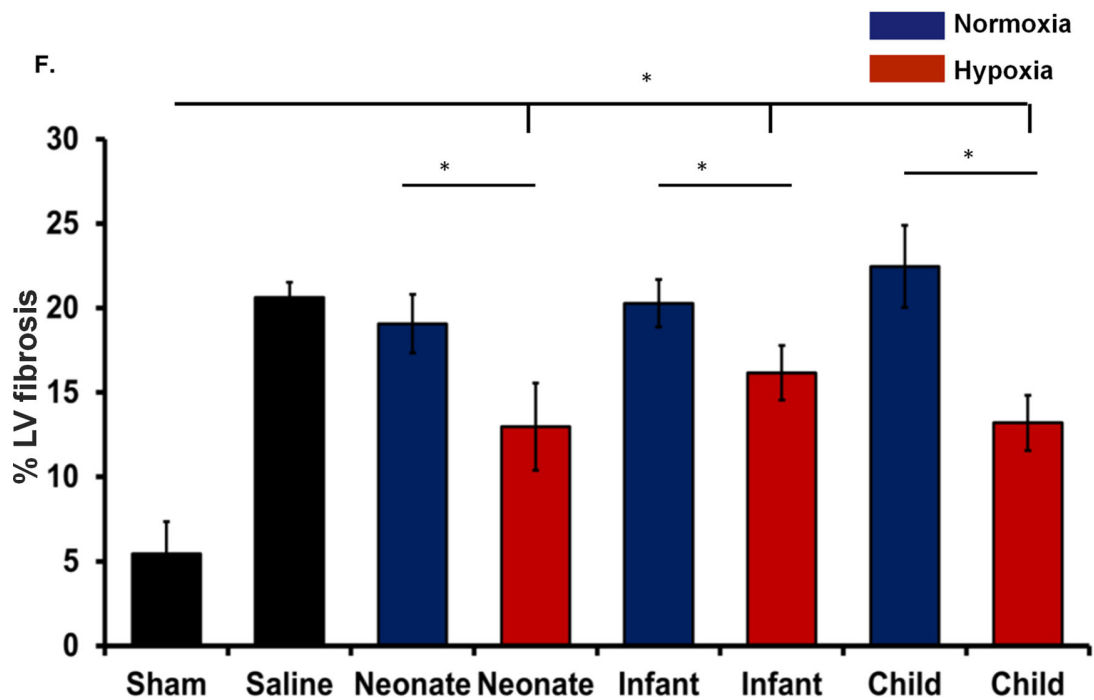
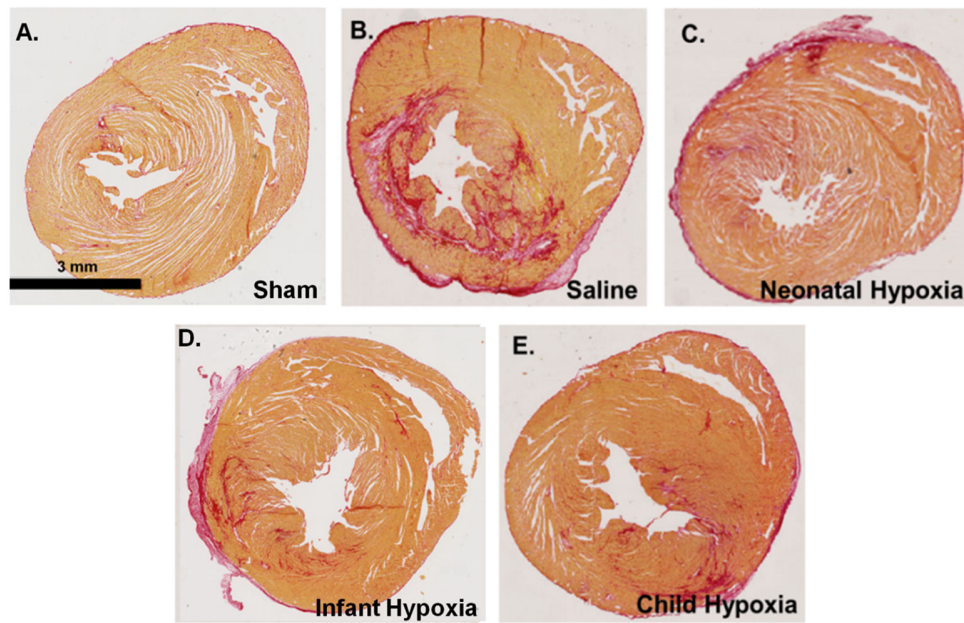


Figure 3. Fibrosis analysis

Picosirius staining of paraffin embedded infarcted hearts. **A–E)** Representative images as labeled. **F)** Grouped data represents mean ± SEM of % LV fibrosis. Hypoxic exosomes from each age group (neonate, infant and child (n=4)) showed significantly decreased fibrosis compared with controls (n=5) and their normoxic counterparts (neonate (n=4), infant (n=5) and child (n=5)). *p<0.05; ANOVA followed by Tukey-Kramer post-test.

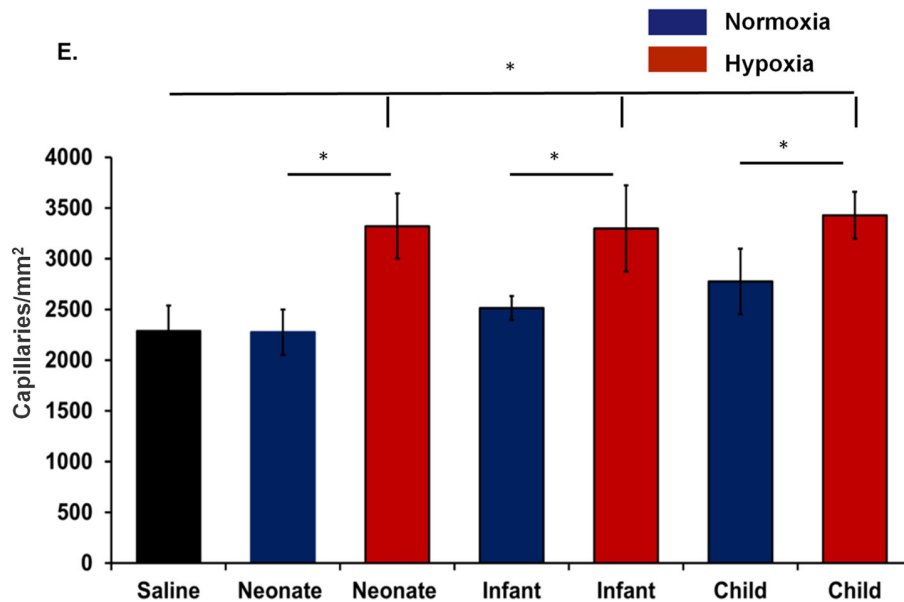
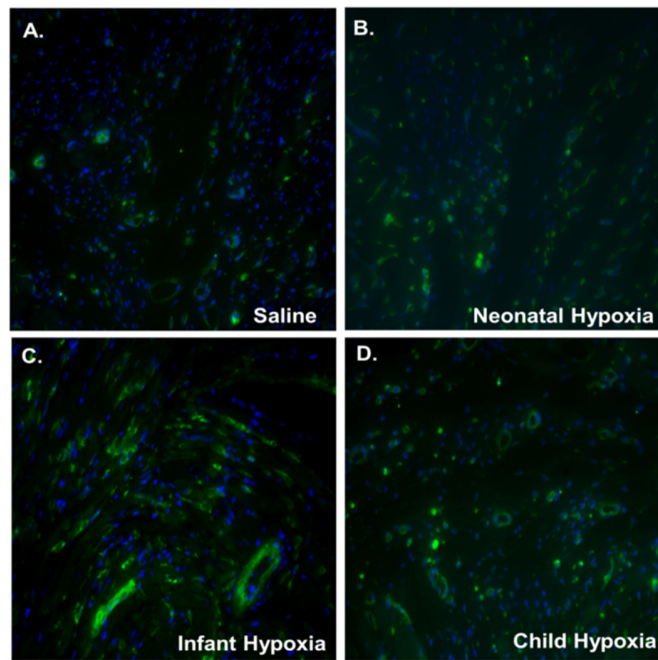


Figure 4. Angiogenesis Analysis

Immunostaining for Isolecetin (Green) and capillary quantification was performed. **A–D**) Representative images as labeled. Capillaries were quantified by counting total number of capillaries per unit area in 3 cross-sectional areas from the infarcted region of LV of each animal. **E**). Grouped data represents mean ± SEM of capillaries/mm². Hypoxic exosomes from each age group (neonate, infant and child(n=4)) showed significantly increased angiogenesis compared with saline-treated controls (n=5) and their normoxic counterparts

(neonate (n=4), infant (n=5) and child (n=5)). *p<0.05; ANOVA followed by Tukey-Kramer post-test.

Author Manuscript

Author Manuscript

Author Manuscript

Author Manuscript

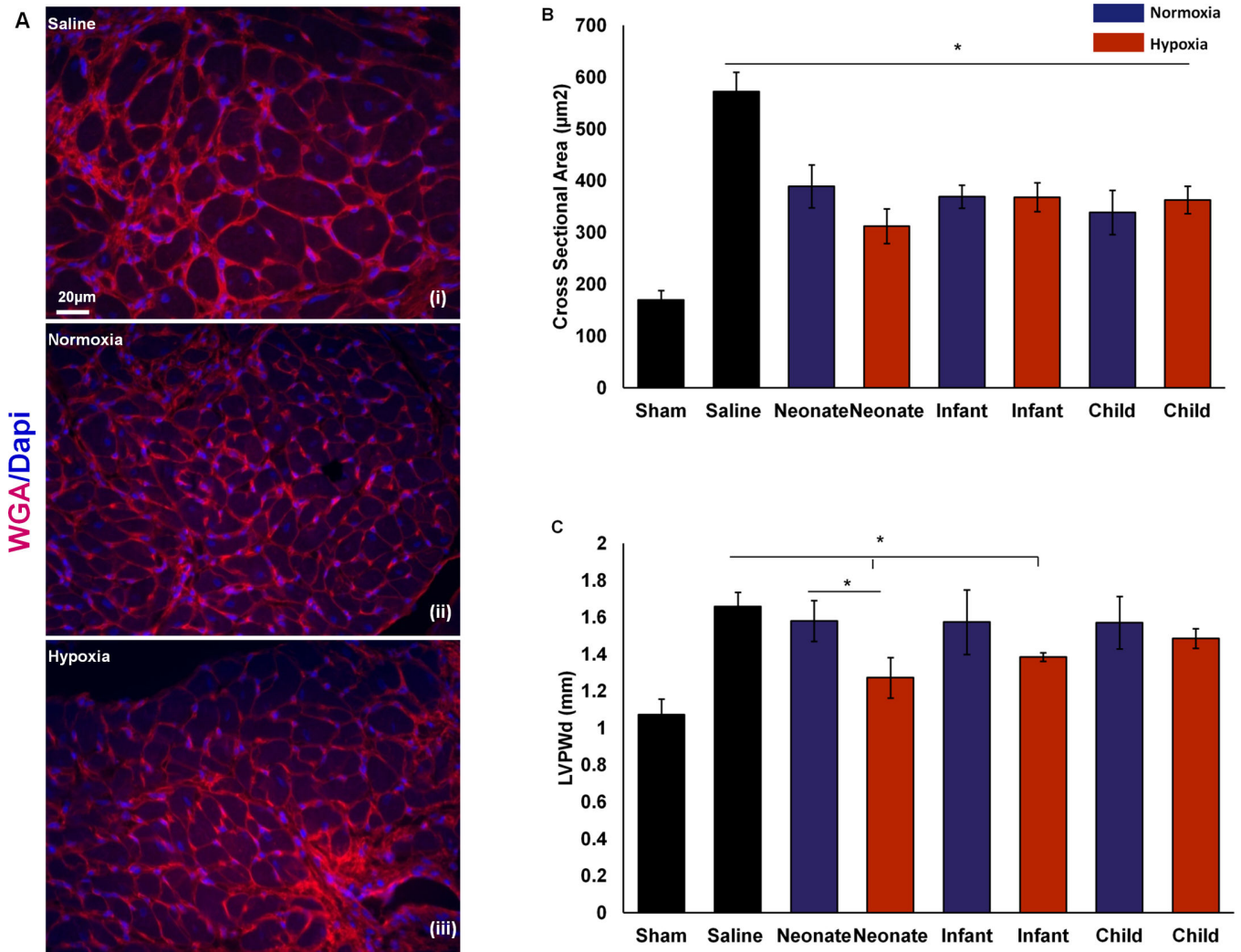


Figure 5. Hypertrophy Analysis

Hypertrophy was analyzed in the peri-infarct region by immunostaining and left ventricular posterior wall diameter (LVPWd) by 2D echo. **A–D**) Immunostaining for wheat germ agglutinin (Red) and nuclei (DAPI) was performed for peri-infarct hypertrophy. Cross-sectional area of cardiac myocytes at the level of the nuclei in-plane in the peri-infarct region was determined at 3 different areas of each animal. **A–C**) Representative images as labeled. **D**). Grouped data represents mean ± SEM of cross section area of a myocyte (µm²). Exosomes from all groups showed significantly decreased hypertrophy compared with control (n=4–5). *p<0.05; ANOVA followed by Tukey-Kramer post-test. **E**) M-mode images of 2D echo were quantified for determining LVPWd. Grouped data represents mean ± SEM of LVPWd. Exosomes from neonatal hypoxia showed significant decreased hypertrophy compared with controls and neonatal normoxia groups. Exosomes from infant hypoxia showed significant decreased hypertrophy compared with controls. *p<0.05; Unpaired t-test.

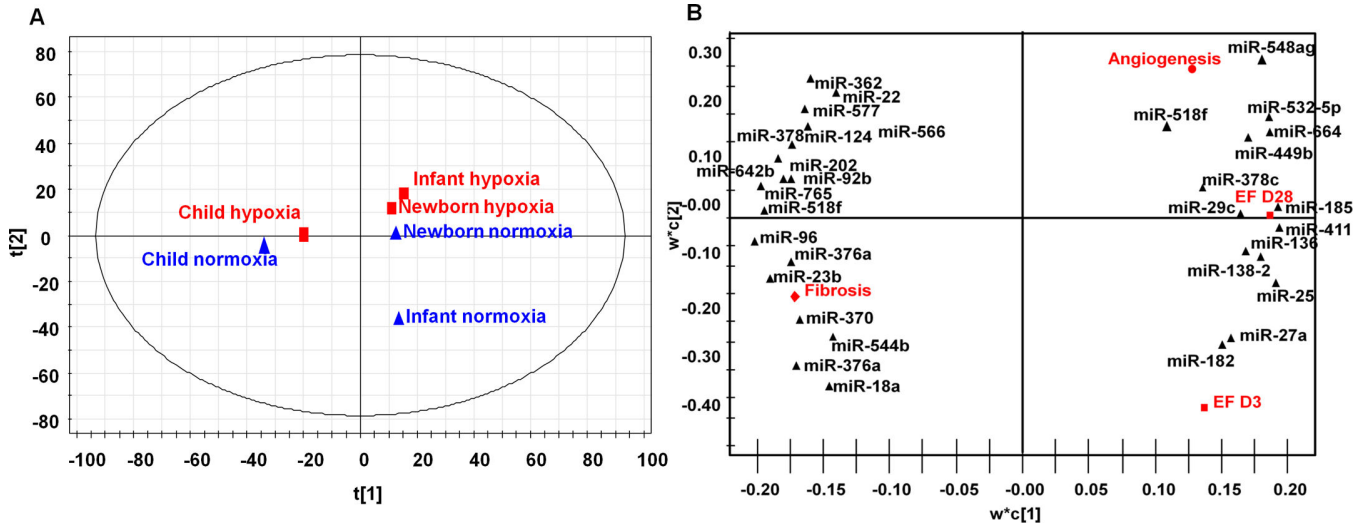


Figure 6. Computational model of exosome study
A) Principal Component (PC) Analysis. All age groups cluster in unique components in the first PC analysis. Hypoxia is predicted to have largest effect. **B) PLSR Analysis.** Top microRNAs with known targets were identified by PLSR and plotted in PC space. Figure represents miR clustering in based upon the outcomes.

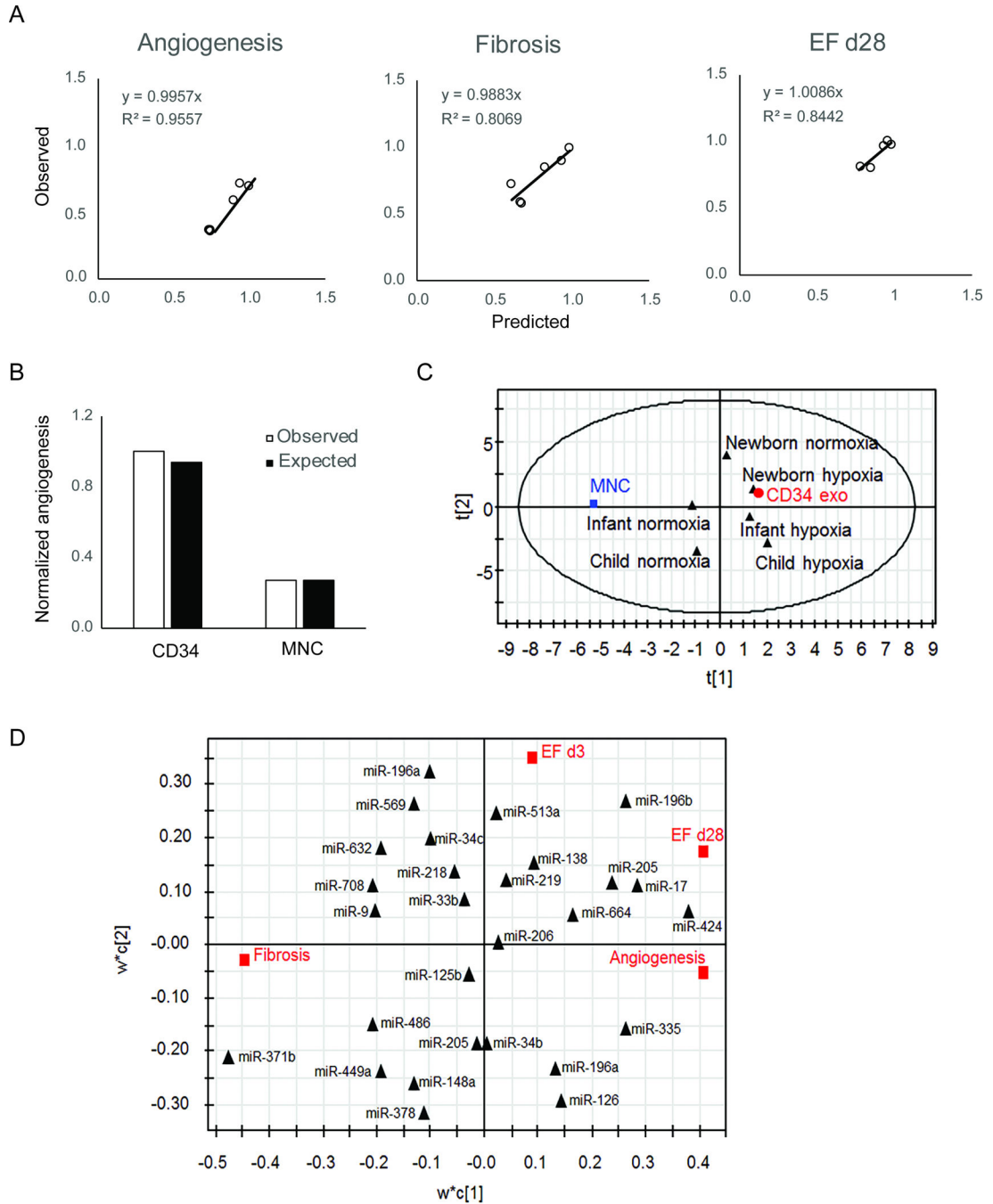


Figure 7. Integrated model with pediatric CPC and CD34+ cell-derived exosomes

A) Predictive model was created using array data and functional data from this study and ref 20 using top 30 microRNAs from Figure 6. **B)** Model results were closely aligned with published studies from (20). **C)** PC analysis of CPC, CD34+ cell, and mononuclear cells (MNCs) showed tight clustering of CD34+ cell-derived exosomes and newborn CPC exosomes. **D)** PLSR analysis identified potential miRNAs from both studies that contribute toward function.

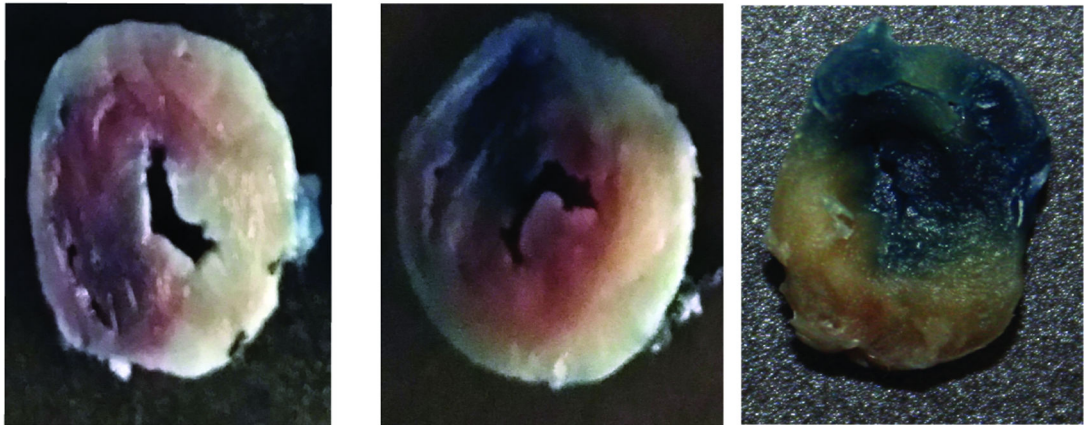
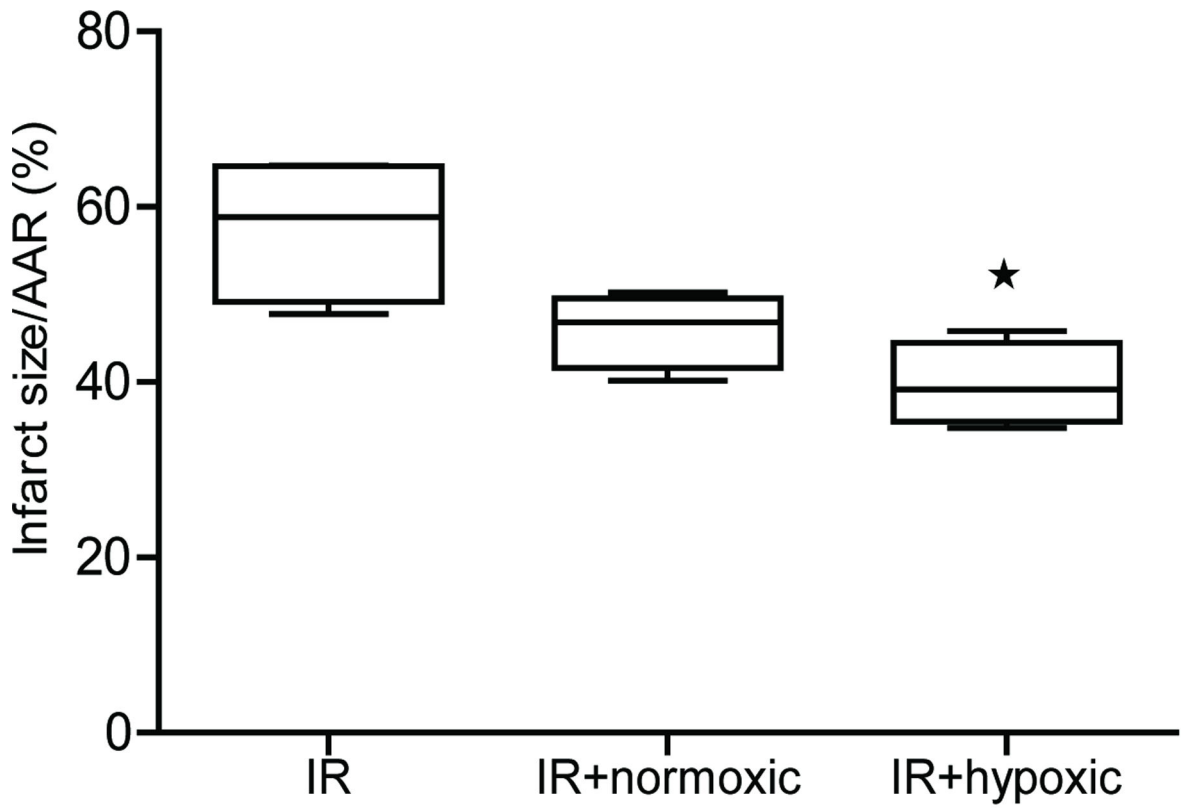


Figure 8. Infarct size in rats treated with newborn exosomes

Top panel shows graph represented as infarct size/area at risk (AAR) in rats treated with saline (IR), or exosomes derived from newborn CPCs cultured under normoxia or hypoxia. Bottom panel shows representative images from the 3 groups. Data are mean \pm SEM (n=4 per group). *p<0.05 ANOVA followed by Tukey-Kramer post-test.